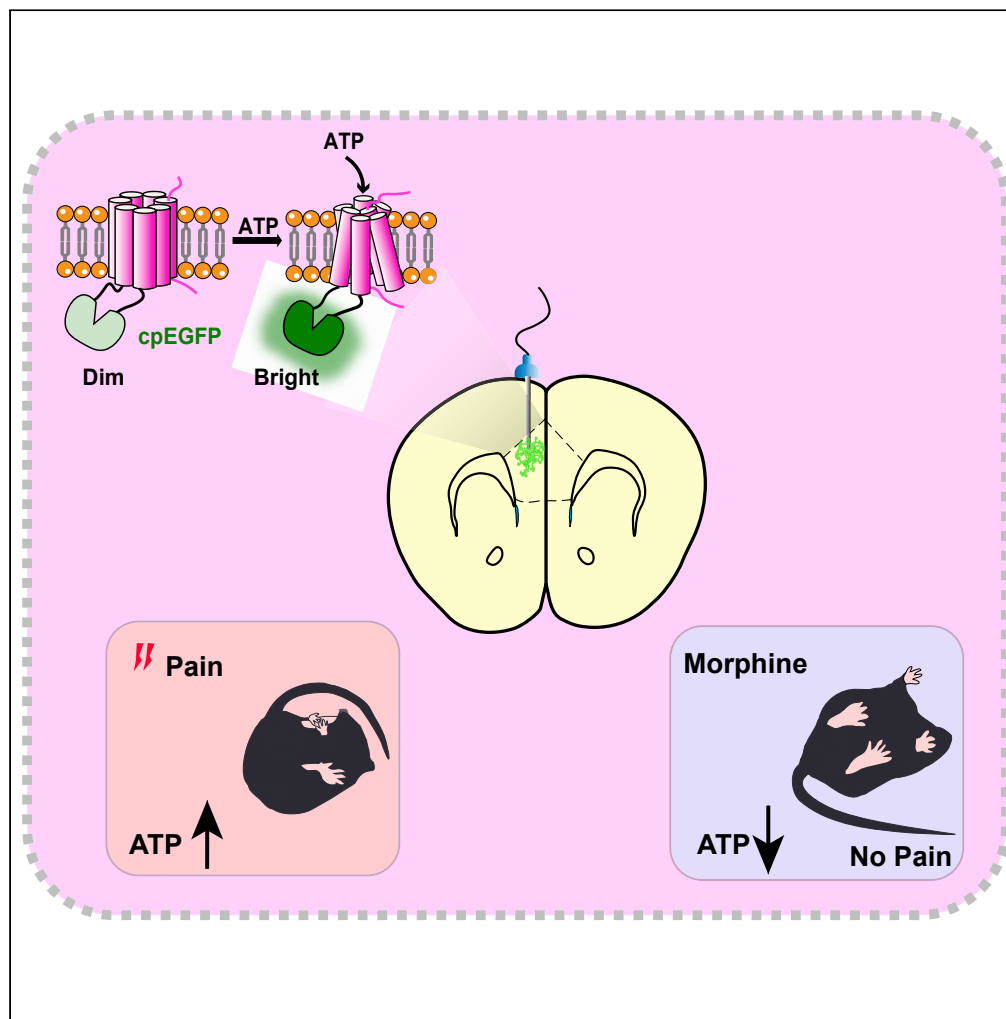# iScience

Article

Reduction of prefrontal purinergic signaling is necessary for the analgesic effect of morphine

Yeting Zeng,
Huoqing Luo,
Zilong Gao, ...,
Yulong Li, Ji Hu,
Jiajun Yang

huji@shanghaitech.edu.cn
(J.H.)
yangjiajunfzy@sina.com (J.Y.)

HIGHLIGHTS

Prefrontal ATP is involved in the analgesic effect of morphine

Blocking P2X7R in the mPFC mimics morphine's analgesic effect

Blocking P2X4R or P2X7R in the mPFC enhances morphine analgesia in tolerant mice

iScience

Article

Reduction of prefrontal purinergic signaling is necessary for the analgesic effect of morphine

Yeting Zeng,[1,11] Huoqing Luo,[2,11] Zilong Gao,[3,4] Xiaona Zhu,[2] Yinbo Shen,[1] Yulong Li,[4,5,6,7] Ji Hu,[2,8,9,10,*] and Jiajun Yang[1,12,*]

SUMMARY

Morphine is commonly used to relieve moderate to severe pain, but repeated doses cause opioid tolerance. Here, we used ATP sensor and fiber photometry to detect prefrontal ATP level. It showed that prefrontal ATP level decreased after morphine injection and the event amplitude tended to decrease with continuous morphine exposure. Morphine had little effect on prefrontal ATP due to its tolerance. Therefore, we hypothesized that the analgesic effect of morphine might be related to ATP in the medial prefrontal cortex (mPFC). Moreover, local infusion of ATP partially antagonized morphine analgesia. Then we found that inhibiting P2X7R in the mPFC mimicked morphine analgesia. In morphine-tolerant mice, pretreatment with P2X4R or P2X7R antagonists in the mPFC enhanced analgesic effect. Our findings suggest that reduction of prefrontal purinergic signaling is necessary for the morphine analgesia, which help elucidate the mechanism of morphine analgesia and may lead to the development of new clinical treatments for neuropathic pain.

INTRODUCTION

Pain management is a major public health burden (Loeser, 2012). Morphine is an opioid drug, commonly used for the relief of moderate to severe pain (Galanie et al., 2015; Kalso et al., 2004; Koshimizu et al., 2018). Anti-nociceptive tolerance is one of the most common adverse effects and is defined as the inability to exert analgesic effect following repeated opioid exposure (Fields and Margolis, 2015). Morphine tolerance is caused by neuroinflammation (Eidson et al., 2017; Zhang et al., 2017) and changes in some important receptors, including the μ-opioid receptor (MOR), N-methyl-D-aspartic acid receptor (NMDAR), and γ-aminobutyric acid receptor (Corder et al., 2017; Dang and Christie, 2012; Martini and Whistler, 2007; Williams et al., 2013). Here we focused on the relationship between morphine and a classical neurotransmitter, adenosine 5′-triphosphate (ATP), which has been widely investigated in recent years (Illes et al., 2019; Kato et al., 2017).

Purinergic signaling plays an important role in the central nervous system (CNS) (Burnstock, 2017) and participates in pain management by mediating the activation of various signal molecules (Jiang et al., 2013; Kasuya et al., 2017; Zhang et al., 2020b). When peripheral or central nerve injury occurs, ATP increased release from damaged neurons. Extracellular ATP subsequently activates purinergic receptors to enhance neuroinflammation by mediating neuronal inflammatory signaling pathways (Chen et al., 2018; Kopp et al., 2019). The critical functions of ATP are mediated via purinergic receptors including P1 receptors and P2 receptors (Burnstock and Kennedy, 1985; Jacobson and Gao, 2006). There are two families of P2 receptors, namely, the P2X family and the P2Y family. The P2X family that is a ligand-gated ion channel consists of P2X (1-7) (Brake et al., 1994; Jarvis and Khakh, 2009). These receptors are widely distributed in the CNS (Burnstock et al., 2011). Given the important role of ATP in pain, inhibiting the release of ATP or affecting the function of the receptors can relieve neuronal inflammation and, thus, the pain response.

The P2X4 receptor (P2X4R) and P2X7 receptor (P2X7R) have been extensively studied in the chronic neuropathic and inflammatory pain (Burnstock and Kennedy, 2011; Duarte et al., 2007; Zhang et al., 2020a). Although immunohistochemical evidences suggested that purinergic receptors were widely distributed in key parts of the brain for pain processing, most studies on the interaction between purinergic receptors

and morphine mainly concentrated on the peripheral nerves or spinal cord. Few studies have investigated the role of purinergic signaling in pain in the medial prefrontal cortex (mPFC). P2X4R and P2X7R in the mPFC changed significantly during the formation of anti-nociceptive tolerance to morphine (Metryka et al., 2019). Owing to the development of optical fiber recording, scientists have detected the dynamic changes of dopamine during morphine addiction and drug resistance (Calipari et al., 2016; Lefevre et al., 2020). At present, the detection of dynamic changes of ATP in the formation of morphine tolerance has not been reported. In this study, an ATP sensor (Wu et al., 2021) is used to explore whether the purinergic signaling in the mPFC is involved in the regulation of morphine analgesia and drug resistance. Our results illustrate that (1) prefrontal purinergic signaling is involved in the analgesic effect of morphine, (2) blocking the prefrontal P2X7R mimics morphine's analgesic effect, and (3) antagonizing the prefrontal P2X4R and P2X7R enhances the analgesic effect of morphine after the development of drug resistance. Our results add a new perspective to the current knowledge on morphine analgesia and tolerance.

RESULTS

Reduction of ATP in the mPFC is involved in the analgesic effect of morphine

We used a genetically encoded G protein-coupled receptor (GPCR)-activation-based (GRAB) sensor for ATP designed by the Li Yulong Lab (Wu et al., 2021) to record extracellular ATP dynamics in the mPFC. The extracellular ATP level is expressed by the fluorescence intensity of green fluorescent protein (Figures 1A and 1B). To quantify changes in ATP dynamics, we used peak analysis to identify transient fluorescent events. By using fiber photometry recordings, we found that intraplantar injection of formalin caused a slow and sustained increase in ATP level (Figure 1C). Meanwhile, morphine (intraperitoneally [i.p.]) significantly decreased the ATP concentrations in the mPFC compared with saline (i.p.) (Figures 1D and 1E).

Event amplitude of ATP in the mPFC tends to decrease with continuous morphine exposure

A single i.p. injection of morphine can cause a decrease of ATP in the mPFC. We used fiber photometry and an ATP sensor to conduct longitudinal measurements of the ATP dynamics in the mPFC during the morphine tolerance developed. The experimental procedures are shown in the Figure 2A. Five mice were repeatedly i.p. injected with morphine (10 mg/kg) for 1 week. Moreover, the signal changes in the mPFC were recorded four times from day 1 and recorded 1 day apart (Days 1, 3, 5, and 7). Interestingly, with repeated morphine administration for 7 days, the inhibition amplitude of ATP in the mPFC tended to decrease. On the last day, the downward trend nearly leveled off (Figures 2B–2F).

Long-term administration of morphine induces tolerance to its analgesic effect. The experimental group received repeated i.p. injection of morphine (10 mg/kg), and the control group was given saline (0.25 mL per mouse) for 7 consecutive days. Both groups underwent formalin tests on Days 1 and 7 (first injection and the final injection) 30 minutes after morphine or saline administration. In the experimental group, the analgesic efficacy of morphine was significantly suppressed at the final injection compared with the first day, indicating the formation of opioid analgesic tolerance (Figure 2G). In comparison, the control group showed no differences in the time of licking and biting of the injected paw between Day 1 and Day 7 (see Figure S1A).

Local infusion of ATP weakens the analgesic effect of morphine

As morphine and pain caused different changes in the ATP levels in the mPFC and morphine had little effects on the prefrontal ATP when the morphine tolerance developed, we hypothesized that the analgesic effect of morphine might be related to ATP. We further explored the relationship between analgesia and the purinergic system by changing the ATP level or affecting its function in the mPFC. We first tested whether the analgesic effect of morphine was abolished by compensating for the decrease of ATP. We directly infused ATP intracerebrally (i.c.) into the mPFC, whereas morphine was infused i.p. (Figures 3A and 3B). In the group injected with morphine plus ATP (0.5 μg per mouse), the anti-nociceptive effect in the formalin test was partially reversed compared with that of the group injected with morphine plus vehicle (Figures 3C and 3D). Infusion of ATP into the mPFC alone neither altered the pain threshold nor exacerbated the pain caused by formalin, so the reduced analgesia of morphine was not caused by the pain increased by ATP injection (see Figures S2A–S2C). However, the analgesic effect of morphine was not completely blocked by the local infusion of ATP. Group morphine plus ATP only achieved 55.6% of the analgesic effect of group morphine alone in the first phase and achieved 72.1% in the second phase. In other words, the analgesic efficiency of morphine in the first phase of the formalin test decreased by 44.4% with ATP infusion and decreased by 27.9% in the second phase. Even if the concentration of ATP
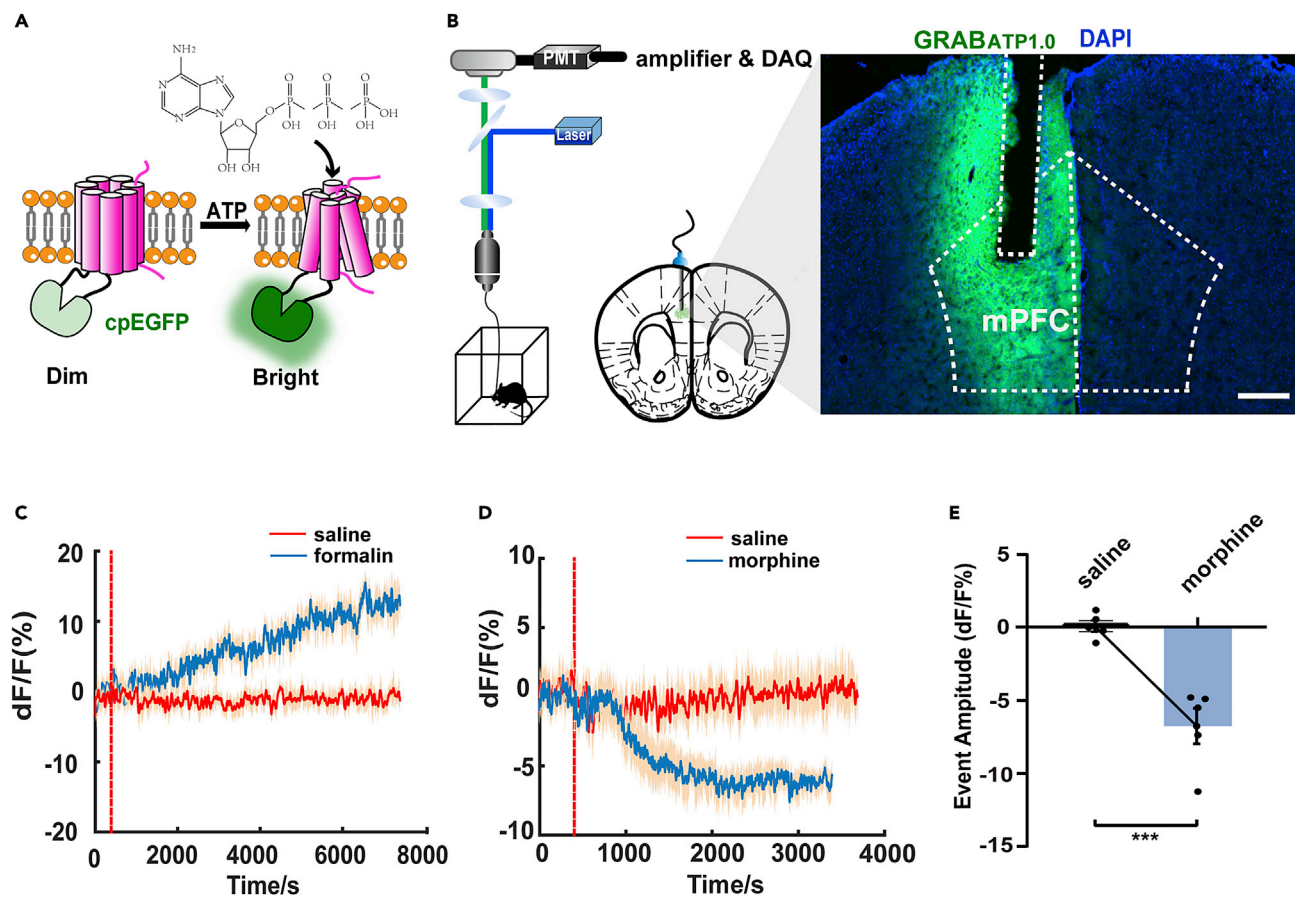
Figure 1. Effects of different stimulants on the ATP concentration in the mPFC

(A) Schematic diagram of the principle of the GRAB-based ATP sensor. Extracellular ATP induces a conformational change in the sensor when binding to the corresponding sites and then increases the fluorescence signal.

(B) Schematic diagram of the optical fiber recording in fluorescence signal changes of the ATP sensor in the mPFC after substance administration in free-moving mice. The location of the adeno-associated virus (AAV) and optical fiber embedded in the mPFC, and a fluorescently stained image showing AAV expression and optical fiber position. Coronal section of the mouse habenula showing expression of ATP (green) and nuclear staining (DAPI, blue). Scale bar, 300 μm.

(C) Changes in the ATP sensor fluorescent signal in the mPFC of the mice after intraplantar injection of saline (0.9% in 20 μL in the red line) or formalin (5% in 20 μL in the blue line). The fluorescence signal changes are denoted by ΔF/F.

(D and E) Changes in the ATP sensor fluorescent signal in the mPFC of the mice after intraperitoneal administration of morphine (10 mg/kg in the blue line) or saline (0.9% in 0.25 mL in the red line). The fluorescent signal changes are denoted by ΔF/F (n = 5, t_8 = 5.399, p = 0.0006, two-tailed, Student's paired t test). Definition of statistical significance: *p < 0.05; **p < 0.01; ***p < 0.001; ****p < 0.0001; ns indicates not significant. Values are reported as the mean ± SEM.

is increased, the blocking efficiency cannot reach 100% (see Figures S3A and S3B). These results suggested that the acute analgesic efficacy of morphine at least partially depends on ATP or purinergic receptors in the mPFC.

Local infusion of BBG into the mPFC mimics morphine's analgesic effect

The supplement of exogenous ATP or the event amplitude of ATP in the mPFC decreases with repeated administration of morphine; it can be proved that the reduction of purinergic signaling molecule is necessary for morphine analgesia. Then we infused purinergic receptor antagonists to block the purinergic function in the mPFC to determine whether it could produce an analgesic effect like morphine. By infusing different types of purinergic receptor antagonists into the mPFC, such as PPADS, TNP-ATP, or BBG, we can not only determine whether purinergic antagonists produce an analgesic effect but also distinguish which receptor is involved in pain transduction. We infused these antagonists 10 minutes before the formalin injection (Figure 4A). The results showed that only BBG caused a reduction in the licking and biting time of the injected paw in response to formalin. BBG could achieve 63.3% of the analgesic efficiency of
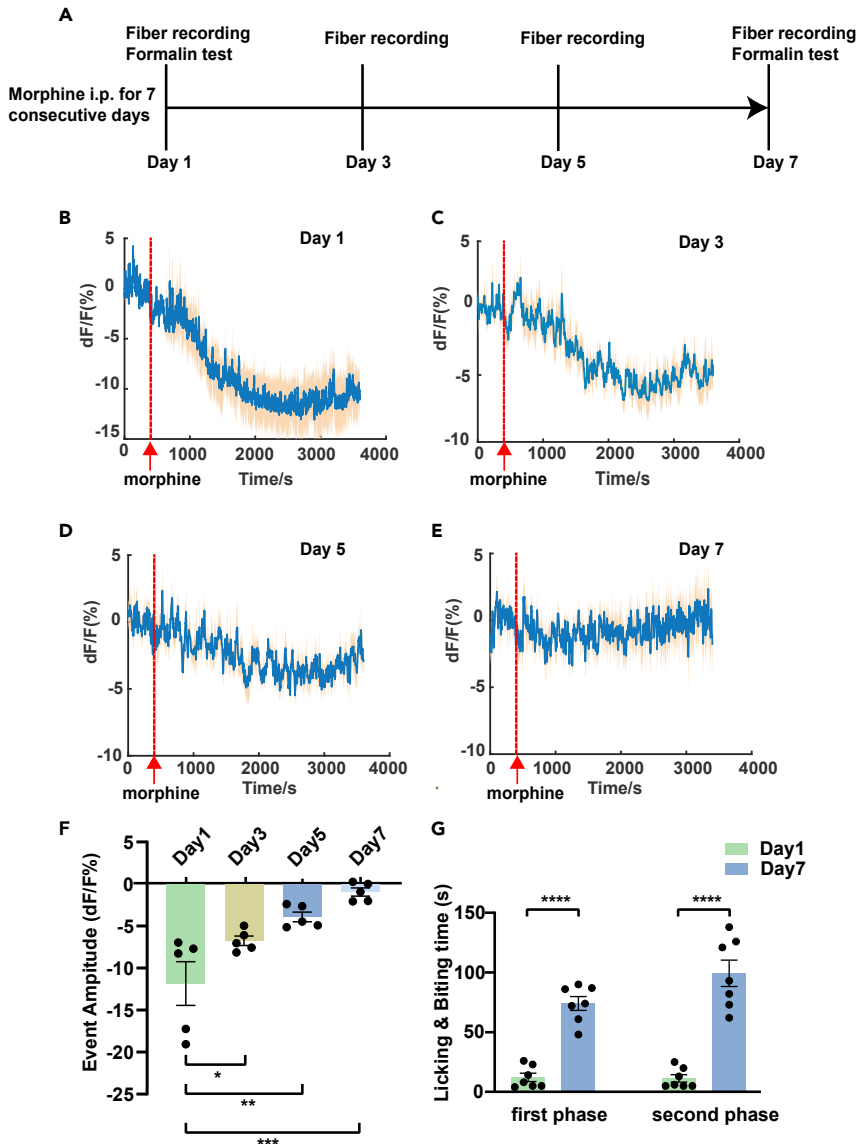
Figure 2. Longitudinal measurements of ATP dynamics in the mPFC during the formation of morphine tolerance

(A) A brief schematic diagram of the steps of morphine tolerance experiment.

(B–E) Changes in the transient fluorescent event in the mPFC when mice were given morphine for 7 consecutive days, including every interval from the first day (Day 1, Day 3, Day 5, and Day 7) (the red line shows the point at which morphine is injected intraperitoneally).

(F) A statistical chart of the variation in the signal recorded for 4 days (n = 5, $F_{3,16}$ = 11.25; p = 0.0012; one-way ANOVA with Tukey's post hoc test; Day 1 versus Day 3: p = 0.0488; Day 1 versus Day 5: p = 0.0025; Day 1 versus Day 7: p = 0.0001).

(G) Changes in analgesic efficacy on Day 1 and Day 7 in the mice given morphine for 7 consecutive days in the first phase (left) (n = 7, t_{12} = 9.156, p < 0.0001, two-tailed, Student's paired t test) and the second phase (right) (n = 7, t_{12} = 7.678, p < 0.0001, two-tailed, Student's paired t test).

Definition of statistical significance: *p < 0.05; **p < 0.01; ***p < 0.001; ****p < 0.0001; ns indicates not significant. Values are reported as the mean ± SEM.

morphine in the first phase and showed no significant difference in the analgesic effect in the second phase. In comparison, neither PPADS nor TNP-ATP showed an effect in the two-phase pain induced by formalin (Figure 4B). Overall, we concluded that P2X7R, but not P2X4R, was involved in acute morphine analgesia. As a P2X7R antagonist, BBG exerted an anti-nociceptive effect in the formalin test.
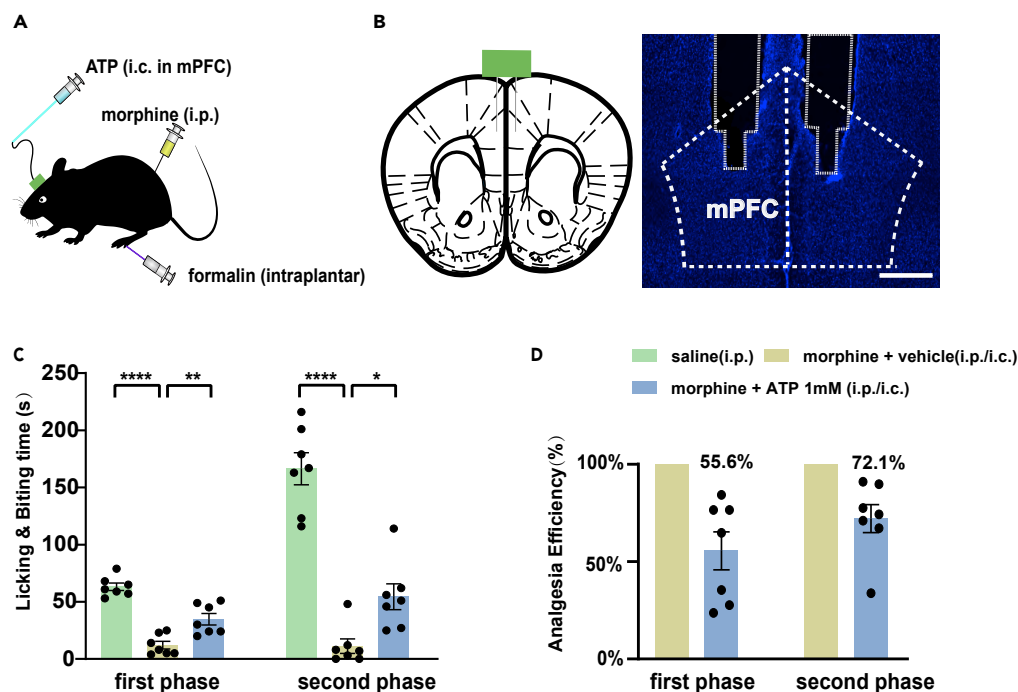
Figure 3. Effects of local infusion of ATP into the mPFC on morphine analgesia

(A) A diagram of the location and mode of administration. ATP was intracerebrally injected into mPFC via a microsyringe (i.c.), morphine was intraperitoneally injected with a common syringe (i.p.), and formalin was intraplantar into the hind paw with a microsyringe (intraplantar).

(B) Schematic diagram of the location of the cannula embedded in the mPFC (left) and a brain slide of the location of cannula insertion in the mPFC (right). Coronal section of the mouse habenula showing nuclear staining (DAPI, blue). Scale bar, 500 μm.

(C) The licking and biting time of the injected paw in formalin test after the administration of morphine (intraperitoneally [i.p.]) and ATP (intracerebrally [i.c.]) into the mPFC in the first phase (left) (n = 7, $F_{2,18}$ = 42.29, p < 0.0001, one-way ANOVA with Tukey's post hoc test; saline versus morphine plus vehicle: p < 0.0001; morphine plus vehicle versus morphine plus ATP: p = 0.0014) and the second phase (right) (n = 7, $F_{2,18}$ = 53.02, p < 0.0001, one-way ANOVA with Tukey's post hoc test; saline versus morphine plus vehicle: p < 0.0001; morphine plus vehicle versus morphine plus ATP: p = 0.0228).

(D) Morphine (i.p.) plus ATP (i.c.) to mPFC achieved 55.6% of the analgesic effect of morphine (i.p.) alone in the first phase and 72.1% in the second phase. In other words, local infusion of ATP antagonized 44.4% of the morphine analgesia in the first phase and antagonized 27.9% in the second phase.

Definition of statistical significance: *p < 0.05; **p < 0.01; ***p < 0.001; ****p < 0.0001; ns indicates not significant. Values are reported as the mean ± SEM.

Local infusion of purinergic receptor antagonists in the mPFC enhances the analgesic efficacy of morphine in morphine-tolerant mice

Previous experiments have shown that P2XR antagonists can produce an analgesic effect (Figure 4B). To confirm whether these antagonists can be used to enhance the analgesic efficacy after the development of morphine tolerance or not we divided the morphine-tolerant mice into four groups (n = 7–8) that received morphine combined with vehicle or three P2XR antagonists (i.p. or i.c.) on the seventh day. Antagonists of P2XRs or vehicle were administered to the mPFC (i.c.) 10 minutes before the i.p. injection of morphine (i.p.) and 40 minutes before the formalin test (see Figure 5A).

The results demonstrated that TNP-ATP and BBG enhanced the analgesic effect of morphine in two phases of the nociceptive response in the formalin pain assay compared with the vehicle. In comparison, PPADS had no effect on morphine analgesic efficacy in the morphine-tolerant mice (Figure 5B). Thus, antagonists of P2X4R and P2X7R can enhance anti-nociceptive effect in morphine-tolerant mice.

DISCUSSION

The human dorsal lateral PFC (the rodent equivalent of the mPFC) plays a vital role in the cognitive and emotional regulation of pain (Devoize et al., 2011; Huang et al., 2019). The neuronal circuit of pain is defined
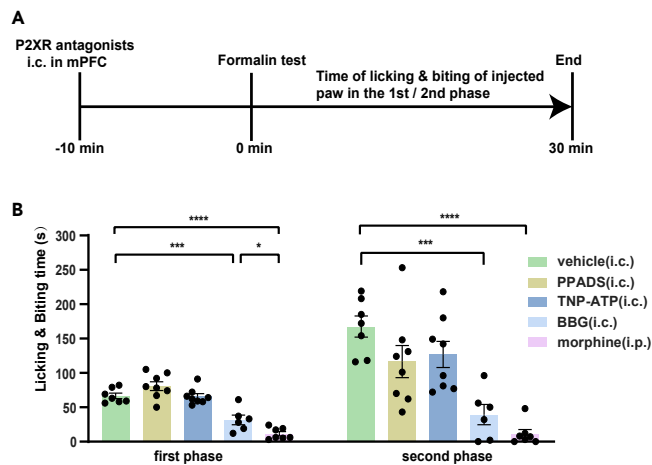
A

P2XR antagonists
i.c. in mPFC

Formalin test

**Time of licking & biting of injected
paw in the 1st / 2nd phase**

End

-10 min   0 min   30 min

B

Figure 4. Effects of antagonists of P2XR in formalin experiments

(A) Simple diagram of the administration sequence.

(B) The local infusion of vehicle or P2XR antagonists into the mPFC caused different reactions to intraplantar injection of formalin.

The licking and biting time of the injected paw in formalin test after the administration of intracerebral P2XR antagonists into the mPFC in the first phase (left) (n = 6–8, $F_{4,31}$ = 31.70, p < 0.0001, one-way ANOVA with Tukey's post hoc test; vehicle versus PPADS: p = 0.2128; vehicle versus TNP-ATP: p > 0.9999; vehicle versus BBG: p = 0.0003; vehicle versus morphine: p < 0.0001); (PPADS versus TNP-ATP: n = 8, t_{14} = 1.990, p = 0.0665, two-tailed, Student's paired t test); (BBG versus morphine: n = 6–7, t_{11} = 2.791, p = 0.0176, two-tailed, Student's unpaired t test). The analgesic effects of BBG (i.c.) into mPFC were 63.3% as effective as morphine (i.p.) in the first phase.

The licking and biting time of the injected paw in the formalin test after the administration of intracerebral P2XR antagonists into the mPFC in the second phase (right) (n = 6–8; $F_{4,31}$ = 13.02, p < 0.0001, one-way ANOVA with Tukey's post hoc test; vehicle vs. PPADS: p = 0.1397; vehicle vs. TNP-ATP: p = 0.2990; vehicle versus BBG: p = 0.0001; vehicle vs. morphine: p < 0.0001); (PPADS versus TNP-ATP: n = 8, t_{14} = 0.3436, p = 0.7363, two-tailed, Student's paired t test); (BBG versus morphine: n = 6–7, t_{11} = 1.845, p = 0.0921, two-tailed, Student's unpaired t test). The analgesic effects of BBG (i.c.) into mPFC were not significantly different from morphine administration (i.p.) in the second phase.

Definition of statistical significance: *p < 0.05; **p < 0.01; ***p < 0.001; ****p < 0.0001; ns indicates not significant. Values are reported as the mean ± SEM.

as the spinal cord-basolateral amygdala-mPFC-periaqueductal gray-locus coeruleus/rostroventral medulla (RVM)-spinal cord (Huang et al., 2019; McGarry and Carter, 2017; Ossipov et al., 2010; Rozeske et al., 2018; Zhang et al., 2020c). Abnormalities in any of these regions may affect the transmission of pain sensation. When P2X7R in the RVM was blocked, experimental animals showed a decrease in bone cancer pain (Huang et al., 2014). As an important relay of the pain transmission center and the upstream afferent nervous system of the RVM, the mPFC is involved in the occurrence and development of neuropathic and inflammatory pain. Furthermore, P2X7Rs are densely distributed in the mPFC (Ková́nyi et al., 2016). Theoretically, affecting the function of P2X7R in the mPFC can also alter the pain response. Our experiment confirmed this conclusion for the first time (Figure 4B). Drug resistance is a major limitation in the clinic. The mPFC is involved in morphine tolerance by sending messages through neuronal connections with the striatum and hippocampus (Delgado et al., 2003; Esmaeili et al., 2012). These two regions are required to regulate the rewarding effects of morphine and the formation of morphine tolerance through the dopamine system (Jordan et al., 2019; Lefevre et al., 2020). It is necessary to carry out a series of studies on the mPFC to investigate morphine analgesia and tolerance.

One major challenge in the development of a purinergic sensor is that the component of extracellular nucleotide signals are at low concentrations, at hundreds of nanomolar to low micromolar levels (Jacobson et al., 2015). Thus, it is difficult to identify the actual ATP level in the brain tissue *in vivo*, both spatially and temporally. This is the first study to conduct longitudinal measurements of ATP dynamics in the mPFC during the development of morphine tolerance. ATP is an energy information substance that is involved in pain (Jiang et al., 2013; Kobayashi et al., 2013). Extracellular ATP binds to P2X or P2Y to regulate neuropathic and inflammatory pain via changes in the phosphorylation of signal molecules (Chang et al., 2007) or the
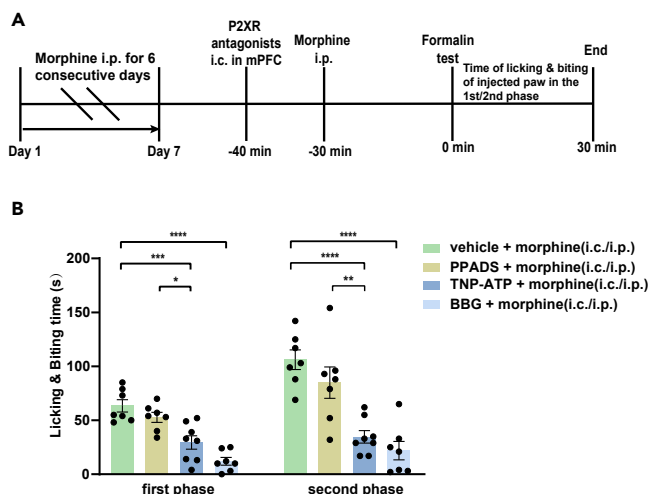
Figure 5. Effects of P2XR antagonists on analgesia in morphine-tolerant mice

(A) A brief schematic of the morphine-tolerant experiment and the schedule of the antagonists and morphine administration after the formation of morphine tolerance on the last day.

(B) Effects of pretreatment with P2XR antagonists (i.c.) into mPFC on morphine analgesia in morphine-tolerant mice. The licking and biting time of the injected paw in formalin test after the pretreatment with P2XR antagonists (i.c.) on tolerant mice in the first phase (left) (n = 7–8, $F_{3,25}$ = 18.98, p < 0.0001, one-way ANOVA with Tukey's post hoc test; vehicle plus morphine versus PPADS plus morphine: p = 0.5033; vehicle plus morphine versus TNP-ATP plus morphine: p = 0.0003; vehicle plus morphine versus BBG plus morphine: p < 0.0001). The licking and biting time of the injected paw in formalin test after the pretreatment with PPADS (i.c.) or TNP-ATP (i.c.) on tolerant mice in the first phase (left) (n = 7–8, t_{13} = 2.943, p = 0.0114, two-tailed, Student's unpaired t test).

The licking and biting time of the injected paw in formalin test after the pretreatment with P2XR antagonists (i.c.) on tolerant mice in the second phase (right) (n = 7–8; $F_{3, 25}$ = 16.60; p < 0.0001; one-way ANOVA with Tukey's post hoc test; vehicle plus morphine versus PPADS plus morphine: p = 0.3177; vehicle plus morphine versus TNP-ATP plus morphine: p < 0.0001; vehicle plus morphine versus BBG plus morphine: p < 0.0001). The licking and biting time of the injected paw in formalin test after the pretreatment with PPADS (i.c.) or TNP-ATP (i.c.) on tolerant mice in the second phase (right) (n = 7–8, t_{13} = 3.377, p = 0.0050, two-tailed, Student's unpaired t test).

Definition of statistical significance: *p < 0.05; **p < 0.01; ***p < 0.001; ****p < 0.0001; ns indicates not significant. Values are reported as the mean ± SEM.

electrical activity of neurons (Khakh and North, 2012). ATP is a danger signal in the CNS and seems to be a mainly slow transmitter/modulator (Illes et al., 2019). It shows a slow and persistent upregulation during sustained damage (Cotrina and Nedergaard, 2009; Rodrigues et al., 2015). Extracellular ATP changes dramatically only if a severe injury occurs, such as a spinal cord injury (Peng et al., 2009). Our results were consistent with this conclusion. With the prolongation of the time, extracellular ATP in the mPFC showed a gradual and slow increase (Figures 1C and S5B) in mice with intraplantar injection of formalin. In recent years, extensive studies have confirmed the pivotal role of ATP in pain. Many chemicals have been used to reduce the neuroinflammatory response and subsequently alleviate neuropathic pain by decreasing ATP release, for example, the inhibitor of vesicular nucleotide transporter (Kato et al., 2017; Yin et al., 2019) and the inhibitor of mammalian target of rapamycin (Cui et al., 2014). The decrease of ATP level in the mPFC may counter nociceptive input and transmission in the CNS. Our results clearly showed that prefrontal ATP participated in pain management. When morphine does not change ATP level in the CNS, the analgesic effect is greatly reduced (Figures 2F, 2G, 3C, and 3D). However, the analgesic effect was not completely blocked. Further research is needed to confirm the key role of the purinergic receptors in the analgesic effect.

P2X7Rs are highly expressed in the mPFC, mostly in glial cells (Inoue and Tsuda, 2009; Scholz and Woolf, 2007). The finding that antagonists of P2X7R exert an analgesic effect has been verified in extensive experiments (Chessell et al., 2005; Ochi-ishi et al., 2014; Xie et al., 2017; Zhou et al., 2019). When purinergic receptors were blocked, experimental animals showed less bone cancer pain (Huang et al., 2014) and diabetic neuropathic pain (Guan et al., 2019). However, the mechanisms of P2X7R in pain are still unclear.

Microglia cells with high expression of P2X7Rs are activated first, and then, astrocytes with a lower level of P2X7Rs are promoted by inflammatory cytokine interleukin (IL)-1 release from microglia (Narcisse et al., 2005). Therefore, P2X7R not only binds to microglia but also acts on astrocytes. The released IL-1 from microglia directly mediates pain sensation through the p-38MAPK pathway (Clark et al., 2010a) or an indirect release of cathepsin (Clark et al., 2010b). By activating P2X7R, extracellular ATP can immediately open potassium channels to increase potassium influx (Ferrari et al., 2006). The increase in potassium ions leads to enhance the release of IL1-β and caspase-1 from macrophages and microglia (Hayashi et al., 2016; Kahlenberg and Dubyak, 2004; Manfredini et al., 2019). These two inflammatory factors, in turn, cause neuroinflammatory and pain responses (Mingam et al., 2008). Chen et al. (2017) found that Pannexin-1, which mediated pore formation, was activated when P2X7R bound to ATP. When P2X7R in the spinal cord is antagonized, it disrupts P2X7R's connection with Pannexin-1 and then reduces the transmission of pain (Bravo et al., 2015). Our finding that the infusion of BBG to the mPFC exerted an analgesic effect (Figure 4B) demonstrated the important role of P2X7R in pain management. In addition to the aforementioned factors, activation of the P2X7R also induces other downstream inflammatory factors associated with the occurrence and maintenance of pain, including COX-2, NADPH oxidase, MIP-1α, TNF-α, and iNOS. These inflammatory factors not only influence the analgesic effect of P2X7R antagonist but also inhibit the analgesic effect of morphine (Puchałowicz et al., 2014; Samad et al., 2001; Takenouchi et al., 2009; Woolf et al., 1997). Experimentally, we also found that infusion of BBG into the mPFC could directly induce the analgesic effect. Therefore, the analgesic effect induced by pretreatment of P2X7R antagonist may be the analgesic effect of BBG itself, or it may be that BBG enhances the sensitivity of mice to morphine (Figures 5B and S4A). More researches are needed to further confirm this conclusion.

We also investigated the role of other purinergic receptors in morphine-tolerant mice. TNP-ATP and PPADS are two types of non-selective P2XR antagonists that activate multiple targets. TNP-ATP blocks the P2X1-7 receptors, whereas PPADS inhibits the P2X1-3 and P2X5-7 receptors (Horvath and DeLeo, 2009). Although PPADS and TNP-ATP can block P2X7R, the blocking efficiency is not high (Donnelly-Roberts and Jarvis, 2007). Besides, other P2X1, 3, 5, 6 receptors are less distributed in the mPFC, so they may not play a major role in the mPFC (Yao et al., 2000). As TNP-ATP has an antagonistic effect on P2X4R, whereas PPADS does not, this difference is often used to explore the role of P2X4R (Horvath and DeLeo, 2009; Xiao et al., 2016). P2X4Rs are distributed on the surface of various glial cells in the mPFC (North and Jarvis, 2013). P2X4Rs are involved in microglial activation and migration (Horvath and DeLeo, 2009; Horvath et al., 2008). Horvath et al. (2010) found that morphine enhanced microglial migration through the PI3K/Akt pathway or in a MOR-dependent manner. Morphine tolerance was significantly reduced with pretreatment of regulators of glial cells, along with a decrease in GFAP and CD11 in the spinal cord (Cui et al., 2008; Raghavendra et al., 2003). This finding indicates that dysfunction of glial cells can abolish morphine analgesia. Other researchers (Tai et al., 2010) found that TNP-ATP alleviated morphine tolerance by regulating the expression of NMDAR subunits and excitatory amino acids, so they concluded that TNP-ATP and NMDAR antagonists acted on the same pathway to influence the opioid analgesic tolerance (Tai et al., 2010). Horvath et al. (2010) found that intracerebral injection of P2X4 receptor antisense oligonucleotide (selectively inhibits the expression of P2X4 receptors) had no effect on the baseline response to mechanical and thermal stimulation, whereas it could inhibit the expression of ED2 to block analgesic tolerance to morphine (Horvath et al., 2010). Furthermore, researchers knocked out the P2X4 gene in mice and found that the acute toxicity and tissue damage caused by intraplantar injection of formalin in P2X4$^{-/-}$ mice was not significantly different from that in normal mice (Tsuda et al., 2009). These results indicate that only with the participation of morphine can P2X4R antagonists maintain the anti-inflammatory and anti-nociceptive effects of morphine in tolerant mice, which corresponded with our results. In our research, two non-selective receptor antagonists, PPADS or TNP-ATP, given alone did not change the licking and biting time of the injected paw compared with the vehicle (Figure 4B). After the formation of morphine tolerance, TNP-ATP restored the analgesic effect of morphine on the seventh day, whereas PPADS did not (Figure 5B). This result showed the crucial role of P2X4R in morphine tolerance, consistent with previous research (Metryka et al., 2019). As the infusion of P2X4R antagonist into the mPFC alone did not induce analgesic effects in morphine-tolerant mice (see Figure S4A), the analgesia of P2X4R antagonist (i.c.) plus morphine may be due to the effect of P2X4R antagonists on morphine sensitivity. In summary, antagonists of P2X4R significantly reduced formalin-evoked nociceptive behaviors, suggesting facilitatory or permissive role for P2X4Rs in the mPFC in inflammatory pain.

In conclusion, our results demonstrated that the reduction of prefrontal ATP was involved in morphine's analgesic effect. The prefrontal ATP level was decreased after morphine administration, and the event amplitude tended to decrease during continuous morphine exposure. The inhibition amplitude nearly disappeared after the development of morphine tolerance. Moreover, the analgesic effect of acute morphine administration was partially revised by local infusion of ATP in the mPFC. So the conclusion was that the acute analgesic effect of morphine mainly depended on P2X7R for the result that selective antagonisting P2X7R mimicked morphine's analgesic effect. Furthermore, inhibitors of P2X4R or P2X7R could increase anti-nociceptive to morphine. Overall, our study thus provides a new perspective for the mechanism of the analgesic effect of morphine and opioid analgesic tolerance.

Limitations of the study

In this study, we used the formalin test as a pain experiment to verify the relationship between purinergic signaling and morphine analgesia. We lack more other pain models to further verify the experimental results. Second, the changes of ATP level in the formation of morphine tolerance also need to be further explored with more technologies and methods.

Resource availability

Lead contact

Jiajun Yang yangjiajunfzy@sina.com

Material availability

This study did not generate any new material.

Data and code availability

The study does not use any unpublished custom code, software, or algorithm that is central to supporting the main claims of the paper.

METHODS

All methods can be found in the accompanying Transparent Methods supplemental file.

SUPPLEMENTAL INFORMATION

Supplemental information can be found online at https://doi.org/10.1016/j.isci.2021.102213.

AUTHOR CONTRIBUTIONS

J.H. and J.Y. designed and supervised this study. Y.Z., H.L., and X.Z. performed the behavioral experiments. Y.S. and Y.Z. performed the experiment of fiber photometry recording and histology. Y.L. designed the genetically encoded ATP sensor. Z.G. helped to analyze the data of fiber photometry. J.H. and Y.Z. wrote the manuscript.

DECLARATION OF INTERESTS

The authors declare no competing interests.

REFERENCES

Brake, A.J., Wagenbach, M.J., and Julius, D. (1994). New structural motif for ligand-gated ion channels defined by an ionotropic ATP receptor. Nature *371*, 519–523.

Bravo, D., Maturana, C.J., Pelissier, T., Hernández, A., and Constandil, L. (2015). Interactions of pannexin 1 with NMDA and P2X7 receptors in central nervous system pathologies: possible role on chronic pain. Pharmacol. Res. *101*, 86–93.

Burnstock, G. (2017). Purinergic signalling: therapeutic developments. Front. Pharmacol. *8*, 661.

Burnstock, G., Fredholm, B.B., and Verkhratsky, A. (2011). Adenosine and ATP receptors in the brain. Curr. Top Med. Chem. *11*, 973–1011.

Burnstock, G., and Kennedy, C. (1985). Is there a basis for distinguishing two types of P2-purinoceptor? Gen. Pharmacol. *16*, 433–440.

Burnstock, G., and Kennedy, C. (2011). P2X receptors in health and disease. Adv. Pharmacol. *61*, 333–372.

Calipari, E.S., Bagot, R.C., Purushothaman, I., Davidson, T.J., Yorgason, J.T., Peña, C.J., Walker, D.M., Pirpinias, S.T., Guise, K.G., Ramakrishnan, C., et al. (2016). In vivo imaging identifies temporal signature of D1 and D2 medium spiny neurons in cocaine reward. Proc. Natl. Acad. Sci. U S A *113*, 2726–2731.

Chang, S.J., Wang, T.Y., Lee, Y.H., and Tai, C.J. (2007). Extracellular ATP activates nuclear translocation of ERK1/2 leading to the induction of matrix metalloproteinases expression in human endometrial stromal cells. J. Endocrinol. *193*, 393–404.

Chen, G., Zhang, Y.Q., Qadri, Y.J., Serhan, C.N., and Ji, R.R. (2018). Microglia in pain: detrimental and protective roles in pathogenesis and resolution of pain. Neuron *100*, 1292–1311.

Chen, S.P., Qin, T., Seidel, J.L., Zheng, Y., Eikermann, M., Ferrari, M.D., van den Maagdenberg, A., Moskowitz, M.A., Ayata, C., and Eikermann-Haerter, K. (2017). Inhibition of the P2X7-PANX1 complex suppresses spreading depolarization and neuroinflammation. Brain *140*, 1643–1656.

Chessell, I.P., Hatcher, J.P., Bountra, C., Michel, A.D., Hughes, J.P., Green, P., Egerton, J., Murfin, M., Richardson, J., Peck, W.L., et al. (2005). Disruption of the P2X7 purinoceptor gene abolishes chronic inflammatory and neuropathic pain. Pain *114*, 386–396.

Clark, A.K., Staniland, A.A., Marchand, F., Kaan, T.K., McMahon, S.B., and Malcangio, M. (2010a). P2X7-dependent release of interleukin-1beta and nociception in the spinal cord following lipopolysaccharide. J. Neurosci. *30*, 573–582.

Clark, A.K., Wodarski, R., Guida, F., Sasso, O., and Malcangio, M. (2010b). Cathepsin S release from primary cultured microglia is regulated by the P2X7 receptor. Glia *58*, 1710–1726.

Corder, G., Tawfik, V.L., Wang, D., Sypek, E.I., Low, S.A., Dickinson, J.R., Sotoudeh, C., Clark, J.D., Barres, B.A., Bohlen, C.J., et al. (2017). Loss of μ opioid receptor signaling in nociceptors, but not microglia, abrogates morphine tolerance without disrupting analgesia. Nat. Med. *23*, 164–173.

Cotrina, M.L., and Nedergaard, M. (2009). Physiological and pathological functions of P2X7 receptor in the spinal cord. Purinergic Signal. *5*, 223–232.

Cui, J., He, W., Yi, B., Zhao, H., Lu, K., Ruan, H., and Ma, D. (2014). mTOR pathway is involved in ADP-evoked astrocyte activation and ATP release in the spinal dorsal horn in a rat neuropathic pain model. Neuroscience *275*, 395–403.

Cui, Y., Liao, X.X., Liu, W., Guo, R.X., Wu, Z.Z., Zhao, C.M., Chen, P.X., and Feng, J.Q. (2008). A novel role of minocycline: attenuating morphine antinociceptive tolerance by inhibition of p38 MAPK in the activated spinal microglia. Brain Behav. Immun. *22*, 114–123.

Dang, V.C., and Christie, M.J. (2012). Mechanisms of rapid opioid receptor desensitization, resensitization and tolerance in brain neurons. Br. J. Pharmacol. *165*, 1704–1716.

Delgado, M.R., Locke, H.M., Stenger, V.A., and Fiez, J.A. (2003). Dorsal striatum responses to reward and punishment: effects of valence and magnitude manipulations. Cogn. Affect. Behav. Neurosci. *3*, 27–38.

Devoize, L., Alvarez, P., Monconduit, L., and Dallel, R. (2011). Representation of dynamic mechanical allodynia in the ventral medial prefrontal cortex of trigeminal neuropathic rats. Eur. J. Pain *15*, 676–682.

Donnelly-Roberts, D.L., and Jarvis, M.F. (2007). Discovery of P2X7 receptor-selective antagonists offers new insights into P2X7 receptor function and indicates a role in chronic pain states. Br. J. Pharmacol. *151*, 571–579.

Duarte, J.M., Oses, J.P., Rodrigues, R.J., and Cunha, R.A. (2007). Modification of purinergic signaling in the hippocampus of streptozotocin-induced diabetic rats. Neuroscience *149*, 382–391.

Eidson, L.N., Inoue, K., Young, L.J., Tansey, M.G., and Murphy, A.Z. (2017). Toll-like receptor 4 mediates morphine-induced neuroinflammation and tolerance via soluble tumor necrosis factor signaling. Neuropsychopharmacology *42*, 661–670.

Esmaeili, M.H., Kermani, M., Parvishan, A., and Haghparast, A. (2012). Role of D1/D2 dopamine receptors in the CA1 region of the rat hippocampus in the rewarding effects of morphine administered into the ventral tegmental area. Behav. Brain Res. *231*, 111–115.

Ferrari, D., Pizzirani, C., Adinolfi, E., Lemoli, R.M., Curti, A., Idzko, M., Panther, E., and Di Virgilio, F. (2006). The P2X7 receptor: a key player in IL-1 processing and release. J. Immunol. *176*, 3877–3883.

Fields, H.L., and Margolis, E.B. (2015). Understanding opioid reward. Trends Neurosci. *38*, 217–225.

Galanie, S., Thodey, K., Trenchard, I.J., Filsinger Interrante, M., and Smolke, C.D. (2015). Complete biosynthesis of opioids in yeast. Science *349*, 1095–1100.

Guan, S., Shen, Y., Ge, H., Xiong, W., He, L., Liu, L., Yin, C., Wei, X., and Gao, Y. (2019). Dihydromyricetin alleviates diabetic neuropathic pain and depression comorbidity symptoms by inhibiting P2X(7) receptor. Front. Psychiatry *10*, 770.

Hayashi, Y., Morinaga, S., Zhang, J., Satoh, Y., Meredith, A.L., Nakata, T., Wu, Z., Kohsaka, S., Inoue, K., and Nakanishi, H. (2016). BK channels in microglia are required for morphine-induced hyperalgesia. Nat. Commun. *7*, 11697.

Horvath, R.J., and DeLeo, J.A. (2009). Morphine enhances microglial migration through modulation of P2X4 receptor signaling. J. Neurosci. *29*, 998–1005.

Horvath, R.J., Nutile-McMenemy, N., Alkaitis, M.S., and Deleo, J.A. (2008). Differential migration, LPS-induced cytokine, chemokine, and NO expression in immortalized BV-2 and HAPI cell lines and primary microglial cultures. J. Neurochem. *107*, 557–569.

Horvath, R.J., Romero-Sandoval, E.A., and De Leo, J.A. (2010). Inhibition of microglial P2X4 receptors attenuates morphine tolerance, Iba1, GFAP and mu opioid receptor protein expression while enhancing perivascular microglial ED2. Pain *150*, 401–413.

Huang, J., Gadotti, V.M., Chen, L., Souza, I.A., Huang, S., Wang, D., Ramakrishnan, C., Deisseroth, K., Zhang, Z., and Zamponi, G.W. (2019). A neuronal circuit for activating descending modulation of neuropathic pain. Nat. Neurosci. *22*, 1659–1668.

Huang, Z.X., Lu, Z.J., Ma, W.Q., Wu, F.X., Zhang, Y.Q., Yu, W.F., and Zhao, Z.Q. (2014). Involvement of RVM-expressed P2X7 receptor in bone cancer pain: mechanism of descending facilitation. Pain *155*, 783–791.

Illes, P., Burnstock, G., and Tang, Y. (2019). Astroglia-derived ATP modulates CNS neuronal circuits. Trends Neurosci. *42*, 885–898.

Inoue, K., and Tsuda, M. (2009). Microglia and neuropathic pain. Glia 57, 1469–1479.

Jacobson, K.A., and Gao, Z.G. (2006). Adenosine receptors as therapeutic targets. Nat. Rev. Drug Discov. 5, 247–264.

Jacobson, K.A., Paoletta, S., Katritch, V., Wu, B., Gao, Z.G., Zhao, Q., Stevens, R.C., and Kiselev, E. (2015). Nucleotides acting at P2Y receptors: connecting structure and function. Mol. Pharmacol. 88, 220–230.

Jarvis, M.F., and Khakh, B.S. (2009). ATP-gated P2X cation-channels. Neuropharmacology 56, 208–215.

Jiang, R., Taly, A., and Grutter, T. (2013). Moving through the gate in ATP-activated P2X receptors. Trends Biochem. Sci. 38, 20–29.

Jordan, C.J., Humburg, B., Rice, M., Bi, G.H., You, Z.B., Shaik, A.B., Cao, J., Bonifazi, A., Gadiano, A., Rais, R., et al. (2019). The highly selective dopamine D(3)R antagonist, R-VK4-40 attenuates oxycodone reward and augments analgesia in rodents. Neuropharmacology 158, 107597.

Kahlenberg, J.M., and Dubyak, G.R. (2004). Mechanisms of caspase-1 activation by P2X7 receptor-mediated K+ release. Am. J. Physiol. Cell Physiol. 286, C1100–C1108.

Kalso, E., Edwards, J.E., Moore, R.A., and McQuay, H.J. (2004). Opioids in chronic non-cancer pain: systematic review of efficacy and safety. Pain 112, 372–380.

Kasuya, G., Yamaura, T., Ma, X.B., Nakamura, R., Takemoto, M., Nagumo, H., Tanaka, E., Dohmae, N., Nakane, T., Yu, Y., et al. (2017). Structural insights into the competitive inhibition of the ATP-gated P2X receptor channel. Nat. Commun. 8, 876.

Kato, Y., Hiasa, M., Ichikawa, R., Hasuzawa, N., Kadowaki, A., Iwatsuki, K., Shima, K., Endo, Y., Kitahara, Y., Inoue, T., et al. (2017). Identification of a vesicular ATP release inhibitor for the treatment of neuropathic and inflammatory pain. Proc. Natl. Acad. Sci. U S A 114, E6297–e6305.

Khakh, B.S., and North, R.A. (2012). Neuromodulation by extracellular ATP and P2X receptors in the CNS. Neuron 76, 51–69.

Kobayashi, K., Yamanaka, H., and Noguchi, K. (2013). Expression of ATP receptors in the rat dorsal root ganglion and spinal cord. Anat. Sci. Int. 88, 10–16.

Kopp, R., Krautloher, A., Ramírez-Fernández, A., and Nicke, A. (2019). P2X7 interactions and signaling - making head or tail of it. Front. Mol. Neurosci. 12, 183.

Koshimizu, T.A., Honda, K., Nagaoka-Uozumi, S., Ichimura, A., Kimura, I., Nakaya, M., Sakai, N., Shibata, K., Ushijima, K., Fujimura, A., et al. (2018). Complex formation between the vasopressin 1b receptor, β-arrestin-2, and the μ-opioid receptor underlies morphine tolerance. Nat. Neurosci. 21, 820–833.

Koványi, B., Csölle, C., Calovi, S., Hanuska, A., Kató, E., Köles, L., Bhattacharya, A., Haller, J., and Sperlágh, B. (2016). The role of P2X7 receptors in a rodent PCP-induced schizophrenia model. Sci. Rep. 6, 36680.

Lefevre, E.M., Pisansky, M.T., Toddes, C., Baruffaldi, F., Pravetoni, M., Tian, L., Kono, T.J.Y., and Rothwell, P.E. (2020). Interruption of continuous opioid exposure exacerbates drug-evoked adaptations in the mesolimbic dopamine system. Neuropsychopharmacology 45, 1781–1792.

Loeser, J.D. (2012). Relieving pain in America. Clin. J. Pain 28, 185–186.

Manfredini, M., Giuliani, A.L., Ruina, G., Gafà, R., Bosi, C., Zoppas, E., Di Virgilio, F., and Bettoli, V. (2019). The P2X7 receptor is overexpressed in the lesional skin of subjects affected by hidradenitis suppurativa: a preliminary study. Dermatology, 1–8.

Martini, L., and Whistler, J.L. (2007). The role of mu opioid receptor desensitization and endocytosis in morphine tolerance and dependence. Curr. Opin. Neurobiol. 17, 556–564.

McGarry, L.M., and Carter, A.G. (2017). Prefrontal cortex drives distinct projection neurons in the basolateral amygdala. Cell Rep. 21, 1426–1433.

Metryka, E., Gutowska, I., Kupnicka, P., Tarnowski, M., Tkacz, M., Listos, J., Talarek, S., Barczak, K., Chlubek, D., and Baranowska-Bosiacka, I. (2019). The expression of purinergic P2X4 and P2X7 receptors in selected mesolimbic structures during morphine withdrawal in rats. Brain Res. 1719, 49–56.

Mingam, R., De Smedt, V., Amédée, T., Bluthé, R.M., Kelley, K.W., Dantzer, R., and Layé, S. (2008). In vitro and in vivo evidence for a role of the P2X7 receptor in the release of IL-1 beta in the murine brain. Brain Behav. Immun. 22, 234–244.

Narcisse, L., Scemes, E., Zhao, Y., Lee, S.C., and Brosnan, C.F. (2005). The cytokine IL-1beta transiently enhances P2X7 receptor expression and function in human astrocytes. Glia 49, 245–258.

North, R.A., and Jarvis, M.F. (2013). P2X receptors as drug targets. Mol. Pharmacol. 83, 759–769.

Ochi-ishi, R., Nagata, K., Inoue, T., Tozaki-Saitoh, H., Tsuda, M., and Inoue, K. (2014). Involvement of the chemokine CCL3 and the purinoceptor P2X7 in the spinal cord in paclitaxel-induced mechanical allodynia. Mol. Pain 10, 53.

Ossipov, M.H., Dussor, G.O., and Porreca, F. (2010). Central modulation of pain. J. Clin. Invest. 120, 3779–3787.

Peng, W., Cotrina, M.L., Han, X., Yu, H., Bekar, L., Blum, L., Takano, T., Tian, G.F., Goldman, S.A., and Nedergaard, M. (2009). Systemic administration of an antagonist of the ATP-sensitive receptor P2X7 improves recovery after spinal cord injury. Proc. Natl. Acad. Sci. U S A 106, 12489–12493.

Puchałowicz, K., Tarnowski, M., Baranowska-Bosiacka, I., Chlubek, D., and Dziedziejko, V. (2014). P2X and P2Y receptors—role in the pathophysiology of the nervous system. Int. J. Mol. Sci. 15, 23672–23704.

Raghavendra, V., Tanga, F., Rutkowski, M.D., and DeLeo, J.A. (2003). Anti-hyperalgesic and morphine-sparing actions of propentofylline following peripheral nerve injury in rats:

mechanistic implications of spinal glia and proinflammatory cytokines. Pain 104, 655–664.

Rodrigues, R.J., Tomé, A.R., and Cunha, R.A. (2015). ATP as a multi-target danger signal in the brain. Front. Neurosci. 9, 148.

Rozeske, R.R., Jercog, D., Karalis, N., Chaudun, F., Khoder, S., Girard, D., Winke, N., and Herry, C. (2018). Prefrontal-periaqueductal gray-projecting neurons mediate context fear discrimination. Neuron 97, 898–910.e896.

Samad, T.A., Moore, K.A., Sapirstein, A., Billet, S., Allchorne, A., Poole, S., Bonventre, J.V., and Woolf, C.J. (2001). Interleukin-1beta-mediated induction of Cox-2 in the CNS contributes to inflammatory pain hypersensitivity. Nature 410, 471–475.

Scholz, J., and Woolf, C.J. (2007). The neuropathic pain triad: neurons, immune cells and glia. Nat. Neurosci. 10, 1361–1368.

Tai, Y.H., Cheng, P.Y., Tsai, R.Y., Chen, Y.F., and Wong, C.S. (2010). Purinergic P2X receptor regulates N-methyl-D-aspartate receptor expression and synaptic excitatory amino acid concentration in morphine-tolerant rats. Anesthesiology 113, 1163–1175.

Takenouchi, T., Sugama, S., Iwamaru, Y., Hashimoto, M., and Kitani, H. (2009). Modulation of the ATP-Induced release and processing of IL-1beta in microglial cells. Crit. Rev. Immunol. 29, 335–345.

Tsuda, M., Kuboyama, K., Inoue, T., Nagata, K., Tozaki-Saitoh, H., and Inoue, K. (2009). Behavioral phenotypes of mice lacking purinergic P2X4 receptors in acute and chronic pain assays. Mol. Pain 5, 28.

Williams, J.T., Ingram, S.L., Henderson, G., Chavkin, C., von Zastrow, M., Schulz, S., Koch, T., Evans, C.J., and Christie, M.J. (2013). Regulation of μ-opioid receptors: desensitization, phosphorylation, internalization, and tolerance. Pharmacol. Rev. 65, 223–254.

Woolf, C.J., Allchorne, A., Safieh-Garabedian, B., and Poole, S. (1997). Cytokines, nerve growth factor and inflammatory hyperalgesia: the contribution of tumour necrosis factor alpha. Br. J. Pharmacol. 121, 417–424.

Wu, Z., He, K., Chen, Y., Li, H., Pan, S., Li, B., Liu, T., Wang, H., Du, J., Jing, M., et al. (2021). An ultrasensitive GRAB sensor for detecting extracellular ATP in vitro and in vivo. bioRxiv. https://doi.org/10.1101/2021.02.24.432680.

Xiao, J., Huang, Y., Li, X., Li, L., Yang, T., Huang, L., Yang, L., Jiang, H., Li, H., and Li, F. (2016). TNP-ATP is beneficial for treatment of neonatal hypoxia-induced hypomyelination and cognitive decline. Neurosci. Bull. 32, 99–107.

Xie, J., Liu, S., Wu, B., Li, G., Rao, S., Zou, L., Yi, Z., Zhang, C., Jia, T., Zhao, S., et al. (2017). The protective effect of resveratrol in the transmission of neuropathic pain mediated by the P2X(7) receptor in the dorsal root ganglia. Neurochem. Int. 103, 24–35.

Yao, S.T., Barden, J.A., Finkelstein, D.I., Bennett, M.R., and Lawrence, A.J. (2000). Comparative study on the distribution patterns of P2X(1)-P2X(6) receptor immunoreactivity in

the brainstem of the rat and the common marmoset (Callithrix jacchus): association with catecholamine cell groups. J. Comp. Neurol. *427*, 485–507.

Yin, Y., Hong, J., Pham, T.L., Shin, J., Gwon, D.H., Kwon, H.H., Shin, N., Shin, H.J., Lee, S.Y., Lee, W.H., et al. (2019). Evans blue reduces neuropathic pain behavior by inhibiting spinal ATP release. Int. J. Mol. Sci. *20*, 4443.

Zhang, W.J., Luo, C., Pu, F.Q., Zhu, J.F., and Zhu, Z. (2020a). The role and pharmacological

characteristics of ATP-gated ionotropic receptor P2X in cancer pain. Pharmacol. Res. *161*, 105106.

Zhang, W.J., Zhu, Z.M., and Liu, Z.X. (2020b). The role and pharmacological properties of the P2X7 receptor in neuropathic pain. Brain Res. Bull. *155*, 19–28.

Zhang, X.Y., Dou, Y.N., Yuan, L., Li, Q., Zhu, Y.J., Wang, M., and Sun, Y.G. (2020c). Different neuronal populations mediate inflammatory pain analgesia by exogenous and endogenous opioids. Elife *9*, e55289.

Zhang, Y., Tao, G.J., Hu, L., Qu, J., Han, Y., Zhang, G., Qian, Y., Jiang, C.Y., and Liu, W.T. (2017). Lidocaine alleviates morphine tolerance via AMPK-SOCS3-dependent neuroinflammation suppression in the spinal cord. J. Neuroinflammation *14*, 211.

Zhou, J., Zhang, X., Zhou, Y., Wu, B., and Tan, Z.Y. (2019). Up-regulation of P2X7 receptors contributes to spinal microglial activation and the development of pain induced by BmK-I. Neurosci. Bull. *35*, 624–636.

Supplemental information

Reduction of prefrontal purinergic

signaling is necessary for the analgesic

effect of morphine

Yeting Zeng, Huoqing Luo, Zilong Gao, Xiaona Zhu, Yinbo Shen, Yulong Li, Ji Hu, and Jiajun Yang
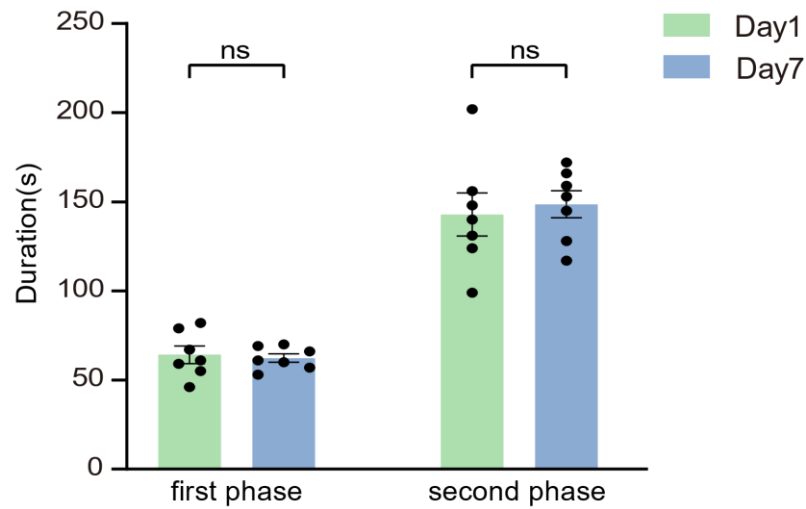
Figure S1

Figure S1. Effects of intraperitoneal injection of saline for seven consecutive days on formalin test. Related to Figure 2.

(A) Mice were intraperitoneally injected with saline for seven continuous days. The licking and biting time of the injected paw by intraplantar of formalin in Day 1 and Day 7 after intraperitoneal injection of saline in the first phase (left) [n=7, t_{12}=0.3423, p=0.7380, two-tailed, Student's paired t test] and in the second phase (right) [n=7, t_{12}=0.4008, p=0.6956, two-tailed, Student's paired t test] were measured. The result indicated that saline injected continuously for seven days didn't alter the pain response in the formalin test.

Definition of statistical significance: p< 0.05; **p < 0.01; ***p < 0.001; ****p < 0.0001; ns indicates not significant. Values are reported as the mean ± SEM.
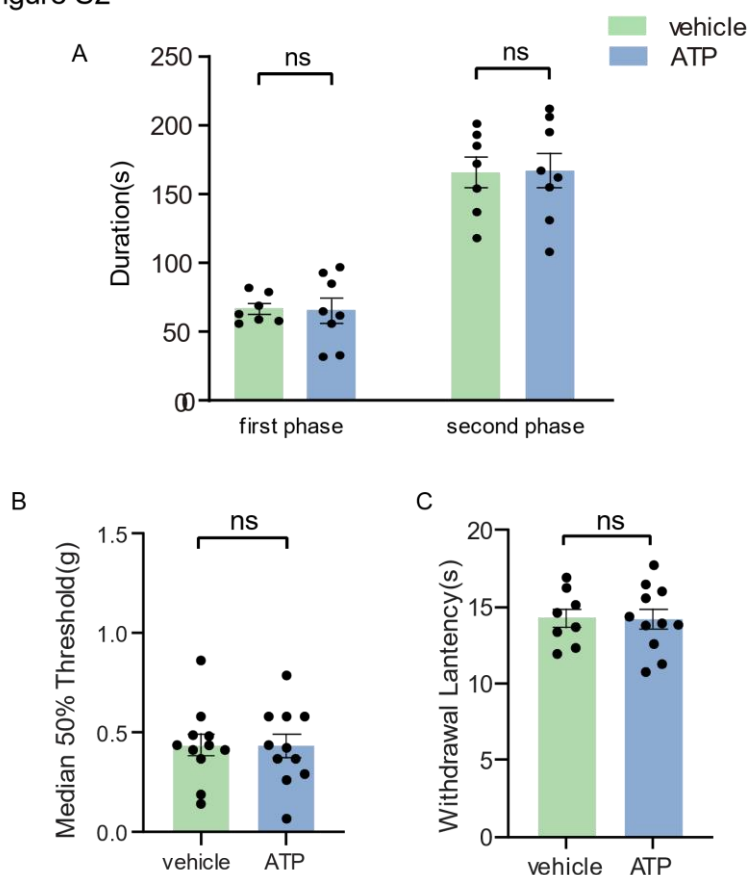
Figure S2

Figure S2. Effects of ATP injections in the mPFC on the baseline pain threshold and formalin-induced pain responses. Related to Figure 3.

(A) The licking and biting time of the injected paw by intraplantar of formalin after intracerebral infusion of ATP or vehicle in the mPFC in the first phase (left) [n=7-8, t_{13}=0.1171, p=0.9085, two-tailed, Student's unpaired t test] and in the second phase (right) [n=7-8, t_{13}=0.07334, p=0.9427, two-tailed, Student's unpaired t test]. There was no change in baseline paw licking and biting time in formalin test by ATP infusion to the mPFC.

(B) Comparison of the results of von Frey test after intracerebral injection of ATP or vehicle into the mPFC [n=11, t_{20}=0.07293, p=0.9426, two-tailed, Student's paired t test]. The results showed that exogenous administration of ATP in the mPFC could not change median 50% threshold.

(C) Comparison of the results of hot plate test after intracerebral injection of ATP or vehicle into mPFC [n=11, 8, t_{17}=0.06954, p=0.9454, two-tailed, Student's unpaired t test]. The results showed that exogenous administration of ATP in the mPFC could not change the withdrawal lantency. Combined with the results above (A-C), administration of exogenous ATP in the mPFC had no effects on the pain threshold of mice, nor did it cause pain response in mice.

Definition of statistical significance: p< 0.05; **p < 0.01; ***p < 0.001; ****p < 0.0001; ns indicates not significant. Values are reported as the mean ± SEM.
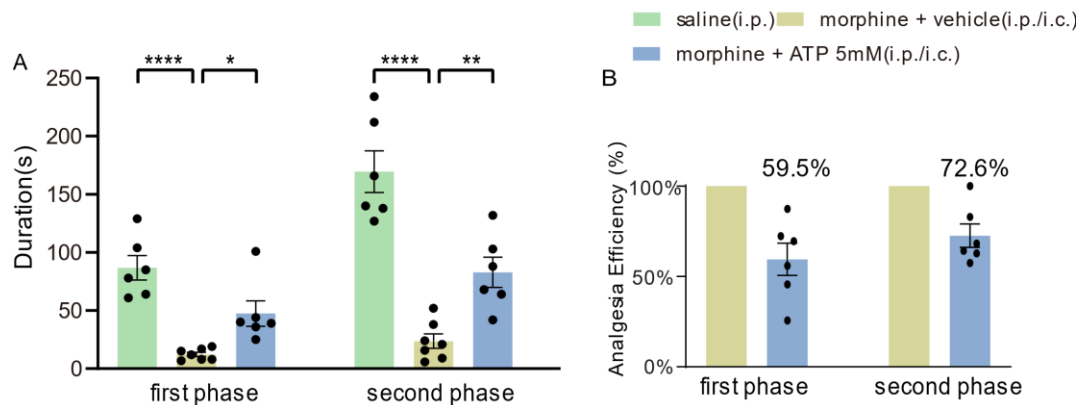
Figure S3

Figure S3. Effects of local infusion of high concentration of ATP (2.5 µg) into the mPFC on morphine analgesia. Related to Figure 3.

(A) The licking and biting time of the injected paw in formalin test after the administration of morphine [intraperitoneally (i.p.)] and ATP [2.5 µg intracerebrally (i.c.)] into the mPFC in the first phase (left) [n=6-7, $F_{2,16}$= 20.17, p<0.0001, one-way ANOVA with Tukey's post hoc test; saline vs. morphine plus vehicle: p<0.0001; morphine plus vehicle vs. morphine plus ATP: p=0.0159] and the second phase (right) [n=6-7, $F_{2,16}$= 33.75, p=0.1522, one-way ANOVA with

Tukey's post hoc test; saline vs. morphine plus vehicle: p < 0.0001; morphine plus vehicle vs.

morphine plus ATP: p=0.0081].

(B) Morphine (i.p.) plus 2.5 µg ATP (i.c.) to mPFC achieved 59.5% of the analgesic effect of morphine (i.p.) alone in the first phase and 72.6% in the second phase. In other words, local infusion of ATP antagonized 40.5% of the morphine analgesia in the first phase and antagonized 27.4% in the second phase.

Definition of statistical significance: p< 0.05; **p < 0.01; ***p < 0.001; ****p < 0.0001; ns indicates not significant. Values are reported as the mean ± SEM.
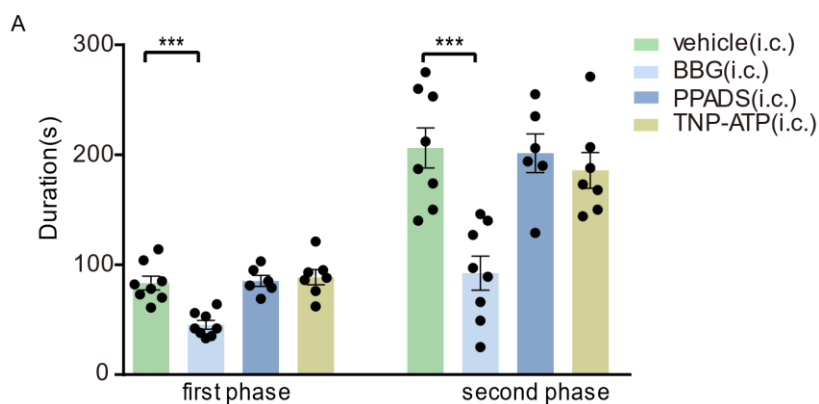
Figure S4

Figure S4. Effects of local infusion of P2XR antagonists into mPFC of morphine-tolerant mice on formalin test. Related to Figure 5.

(A) The licking and biting time of the injected paw in formalin test after the treatment of P2XR

antagonists (i.c.) in the tolerant mice in the first phase (left) [n=6–8, $F_{3,\,25}$=13.81, p<0.0001, one-way ANOVA with Tukey's post hoc test; vehicle vs. BBG: p=0.0001; vehicle vs. PPADS p=0.9908; vehicle vs. TNP-ATP: p=0.8420]. The licking and biting time of the injected paw in formalin test after the treatment of PPADS (i.c.) or TNP-ATP (i.c.) in the tolerant mice in the first phase (left) [n=6-7, t_{11}=0.3868, p=0.7063, two-tailed, Student's unpaired t test].

The licking and biting time of the injected paw in formalin test after the treatment of P2XR antagonists (i.c.) in the tolerant mice in the second phase (right) [n=6–8, $F_{3,\,25}$=10.46, p=0.0001, one-way ANOVA with Tukey's post hoc test; vehicle vs. BBG: p=0.0001; vehicle vs. PPADS p=0.9946; vehicle vs. TNP-ATP: p=0.7243]. The licking and biting time of the injected paw in formalin test after the treatment of PPADS (i.c.) or TNP-ATP (i.c.) in the tolerant mice in the second phase (right) [n=6-7, t_{11}=0.6486, p=0.5299, two-tailed, Student's unpaired t test].

Definition of statistical significance: p< 0.05; **p < 0.01; ***p < 0.001; ****p < 0.0001; ns indicates not significant. Values are reported as the mean ± SEM.

Figure S5

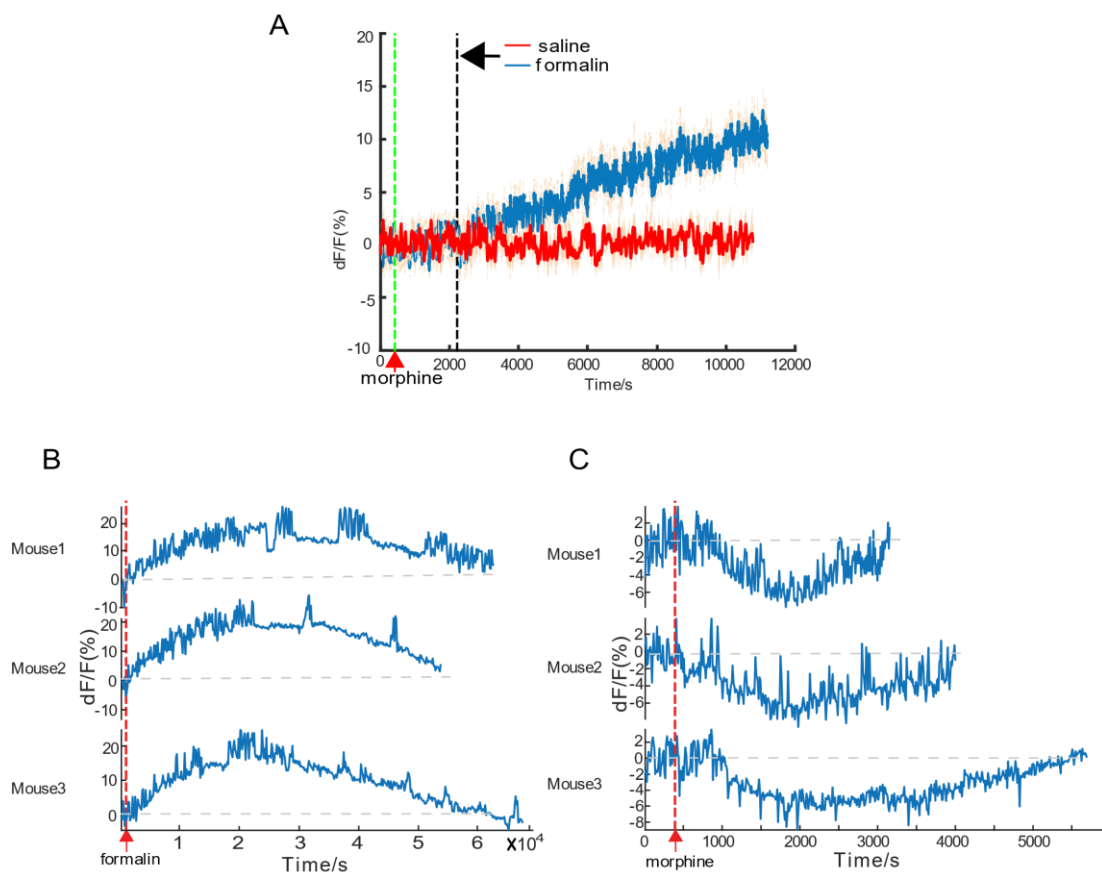**Figure S5. Effects of formalin injection on the concentration of ATP in the mPFC of morphine-tolerant mice. Related to Figure 1, 2.**

(A) In morphine-tolerant mice, paw licking and biting behaviors were observed in formalin mice half an hour after morphine administration as morphine analgesic effect decreased, and the fluorescence signal was increased. (The green dashed line shows the time of intraperitoneal

injection of morphine in morphine-tolerant mice. The black dashed line shows the changes in fluorescence signals caused by the intraplantar injection of saline or formalin in mice's hind paw in half an hour after the injection of morphine.)

(B) After intraplantar injection of formalin, the ATP into the mPFC showed a slow but sustained increase, which began to decrease after 6 hours to 9 hours and returned to the baseline level after 16 hours to 19 hours (The red dashed line indicates the time to intraplantar injection of formalin).

(C) After intraperitoneal administration of morphine, ATP in the mPFC decreased, and the fluorescence signal returned to baseline 40 minutes to 1.5 hours later. (The red dashed line indicates the time to intraperitoneal injection of morphine.)

Transparent Methods

Animals

Adult male and female C57BL/6J mice (aged 8-12 weeks) purchased from Shanghai Model Organisms (Shanghai, China) were used. Male and female mice were used for fiber photometry recording in vivo, and male mice were used for behavioral experiments. Mice were housed 4-5 per cage at 22-25 °C under a 12-h/12-h light/dark cycle (light on from 21:00 to 9:00) with free access to food and water and were randomly allocated to different test groups. Experiments were performed exactly as approved by the Institutional Animal Care and Use Committee (IACUC) of Shanghai Jiaotong University and ShanghaiTech University.

Materials

Morphine (Northeast Pharmaceutical Group Shenyang First Pharmaceutical Co., Ltd. Shenyang China), ATP (Sinopharm Rongsheng Pharmaceutical Co., Ltd. Henan China), selective P2X7R antagonist: Brilliant Blue G (BBG, Sigma), non-selective P2X receptor (P2X1-3, 5-7 receptor) antagonists: pyridoxal phosphate-6-azo (benzene-2,4-disulfonic acid) tetrasodium salt hydrate (PPADS, Sigma), non-selective P2X receptor (P2X1-7 receptor) antagonists: the ATP analog 2′,3′-0-(2,4,6-trinitrophenyl)-adenosine 5′-triphosphate triethylammonium salt (TNP-ATP, Tocris), and formalin (Beijing Solarbio Science & Technology Co., Ltd. Beijing China) were used.

Viral microinjection and stereotactic surgery

GRAB$_{ATP}$ (1.89×10^{13} genomic copies per ml) was designed in Li Yulong Lab (Wu et al.,2021)

. Optical fiber and cannula were purchased from RWD Life Science Co., LTD (Shenzhen China). Stereotaxic surgeries were performed as previously described (Zhang et al., 2020; Li et al., 2020; Qiu et al., 2020). The mice were anesthetized with an intraperitoneal injection of pentobarbital (100 mg/kg) and kept warm (37°C) with an electric heating pad (BrainKing Biotech). Then, the mice were placed in a stereotaxic apparatus (RWD Instruments, Shenzhen, China) to keep their skulls parallel to the reference panel. Next, 300 nl of AAV virus was slowly microsyringe injected (60 nl /min) by a glass pipette from a small hole (15-25 μm in diameter) into the unilateral mPFC (coordinates from the bregma: -1.6 mm AP, -0.3 mm ML, 2.0 mm DV). The pipette remained in place for at least ten minutes after the injection. The coordinate of the fiber was 0.15 mm above the viral sites. The optical fiber was then fixed with dental cement (RWD Life Science Co., Ltd.).

For the implantation of the microinjection cannula in the mPFC, the procedure was the same as described before but without AAV virus injection (coordinates from the bregma: -1.6 mm AP, ±0.3 mm ML, 1.8 mm DV).

The locations of the virus, fiber, or microinjection in the mPFC were defined by visualization of stained tissue under a microscope.

Fiber photometry recording

After 2 weeks for recovery, fiber photometry recordings were conducted in the open-field chambers described before (Lefevre et al., 2020; Wang et al., 2020). Continuous fiber photometry recordings were conducted before and after substances administration. For chronic morphine treatment, continuous fiber photometry recordings were conducted before and after morphine administration on days 1, 3, 5, 7 and the spontaneous fluorescent transient events were detected.

Fluorescence signals were obtained with a fiber photometry system (488 nm excitation laser, 505-544 nm emission filter, and a photomultiplier tube). The analog voltage signals were digitalized at 100 Hz and recorded by a Power 1401 digitizer and Spike2 software (CED, Cambridge, UK). The laser power was adjusted to 20-40 μW to minimize bleaching.

The photometry data were exported to MATLAB R2020b mat files. We calculated the values

of fluorescence change (ΔF/F) by (F−F0)/F0, where F0 was the baseline fluorescence signal averaged over a 400- seconds-long control time window. The ΔF/F values are presented with a blue or red average plot indicating the average of the several yellow curves that represented the signal variation through trial and error. We collected the mean ΔF/F values 400 seconds before agent injection and the mean ΔF/F values after agent injection as the control or the treatment values. For the implantation of the microinjection cannula into mPFC, the procedure was the same as described before but without AAV virus injection.

Drug exposure

The procedure for intracerebral injection follows the steps described previously (Tsuda et al., 1999b). For fiber photometry recording experiment (Figure 1), formalin (5% in 20 µl) or saline (0.9% in 20 µl) was injected into hind paw (Figure 1C) and morphine (10 mg/kg) or saline (0.9% in 0.25 ml) was intraperitoneally (Figure 1D, E). Intraperitoneal injection of morphine (10 mg/kg) or saline (0.9% in 0.25 ml) was followed by formalin test in thirty minutes. In the chronic morphine tolerance experiment, the mice were given morphine (10 mg/kg) once a day for seven consecutive days to develop anti-nociceptive tolerance as described previously (Koshimizu et al., 2018; Shu et al., 2006; Zhang et al., 2018). Five mice with ATP sensor and fiber in the mPFC were used for fiber photometry recording. Continuous fiber photometry recordings were conducted before and after morphine administration on days 1, 3, 5, and 7. Seven mice were performed the formalin test thirty minutes after morphine administration on days 1 and 7 to assess the formation of opioid tolerance. To testify the real relationship between the morphine and ATP, we intraperitoneally (i.p.) injected with morphine followed by infusion of ATP (0.5 µg per mouse) or vehicle (1.0 µl per mouse). The saline was injected intraperitoneally as control group (see Figure S1A). All groups performed formalin test after assays administration. In acute analgesic experiments (Figure A, B), the formalin test was performed ten minutes after infusion of substances to mPFC via indwelling intracerebral catheter. Intracerebral dosing into mPFC consisted of intracerebral administration of vehicle (1 µl per mouse), PPADS (0.2 µg per mouse), TNP-ATP (0.2 µg per mouse), and BBG (42.7 µg per mouse). For the chronic morphine experiment, the morphine tolerant mice were divided into four groups pretreated with different antagonists into mPFC. The mPFC was infused with vehicle or purinergic antagonists ten

minutes before morphine administration on day 7 (Figure 5A). The formalin test was performed thirty minutes after morphine injection. The substances were infused slowly into the corresponding brain region, and the entire injection process lasted one minute. After injection, the needle tube remained for at least another minute.

Behavioral assays

Behavioral tests were performed during the dark phase (9:00-21:00). Three days before the experiment, all mice were handled for at least five minutes per day. The mice were placed in the experimental room for three hours before the tests. Then, the mice were placed in an experimental container for half an hour before the experiment.

Formalin test

Mice received an intraplantar injection of 20 µl of formalin (5% diluted in 0.9% sterile saline) in the hind paw with a microliter syringe as described previously (Chen et al., 2019; Hussey et al., 2007; Magnúsdóttir et al., 2018). For the group given morphine alone, the mice were given formalin thirty minutes after morphine injection. Following formalin injection, the mice were immediately returned to the observation chamber (10 cm x 10 cm x 15 cm) with opaque sides and transparent bottoms and the observation time started. In experiments with the antagonists, mice were given intracerebrally ten minutes before the formalin pain assay. The animal behaviors were recorded by a video camera located beneath the observation chamber for a period of at least thirty minutes. The videos were recorded for subsequent analysis. Formalin injection causes intense licking and biting of the injected paw in two phases. The first phase was defined as acute neurogenic pain occurring within the first five minutes after the intraplantar injection of formalin. The second phase is chronic peripheral tonic inflammation pain and occurs 15-30 minutes after formalin administration. The licking and biting of the injected paw in two phases is considered a sign of nociception.

Morphine treatment

Adult male mice (aged 8-12 weeks) were used for the morphine tolerance experiment. The protocol conducts as described previously (Koshimizu et al., 2018; Shu et al., 2006; Zhang et al., 2018). Mice were intraperitoneally injected with morphine (10 mg/kg) daily for one week. To assess morphine tolerance, formalin test was carried out 30 minutes after injection of morphine on the first and seventh days. When morphine tolerance developed, the analgesic effect of

morphine on the pain caused by formalin was significantly reduced (Figure 2G).

Von Frey Test

The procedure is the same as described before (Chen et al., 2019, Young et al., 2016). Von Frey Filaments (von Frey hair, Stoelting, Wood Dale, USA) were used in this test. Mice were placed in a plastic chamber (4cm x 4cm x 7cm) with a metal mesh bottom for 20 minutes for behavioral accommodation. Mechanical sensitivity was performed on the hind paw plantar surface. The paw was touched by one hair for several seconds and take a break for more than 10 seconds. The up and down methods were used to determine the bending force causing the median 50% withdrawal (Chaplan et al., 1994).

Hot plate test

Heat sensitivity was determined with a hot plate (BIOSEB, German). The hot plate test was performed as described as before (McCoy et al., 2013). The latency to licking a hind paw, jump, or shake hind paw were measured with a 30 seconds cut-off time.

Histology

The procedure for immunofluorescence staining follows the steps described previously (Yuan et al., 2019). Animals were deeply anesthetized by intraperitoneal injection of pentobarbital (100 mg/kg) and perfused with phosphate-buffered solution (PBS, pH 7.4) followed by 4% paraformaldehyde (PFA). Then, the head was removed and soaked in 4% PFA overnight. After dissection, the brain was cryoprotected in 20% sucrose in PBS at 4°C overnight. Coronal sections (40 μm thick) containing the mPFC were obtained by a cryostat microtome. The slides were washed with 0.1 M PBS buffer three times. Finally, 4',6- diamidino-2-phenylindole (DAPI) were used to seal the slides. For the fluorescent images, an Olympus VS120 microscope was used to take the photos. The mPFC brain section containing the $GRAB_{ATP}$ and fiber channel is shown in Figure 1B.

Data analysis

ImageJ software was used to process the brain slides. All statistical analyses were performed with GraphPad Prism 8.0 or MATLAB R2020b. Intergroup comparisons of different results were performed using Student's paired / unpaired t-test and one-way analysis of variance (ANOVA). Definition of statistical significance: $p < 0.05$; $**p < 0.01$; $***p < 0.001$; $****p < 0.0001$; ns

indicates not significant. All summary data are displayed as the mean ± SEM.

Supplemental References

Zhaofa Wu., Kaikai He., Yue Chen., Hongyu Li., Sunlei Pan., Bohan Li., Tingting Liu., Huan W
an., Jiulin Du., Miao Jing., Yulong Li. An ultrasensitive GRAB sensor for detecting extracellular
ATP in vitro and in vivo. bioRxiv, 2021.02.24.432680

doi: https://doi.org/10.1101/2021.02.24.432680

Zhang, X., Lei, B., Yuan, Y., Zhang, L., Hu, L., Jin, S., Kang, B., Liao, X., Sun, W., Xu, F., et al.
(2020). Brain control of humoral immune responses amenable to behavioural modulation.
Nature 581, 204-208.

Li, J., Lu, C., Gao, Z., Feng, Y., Luo, H., Lu, T., Sun, X., Hu, J., and Luo, Y. (2020). SNRIs
achieve faster antidepressant effects than SSRIs by elevating the concentrations of dopamine
in the forebrain. Neuropharmacology 177, 108237.

Qiu, G., Wu, Y., Yang, Z., Li, L., Zhu, X., Wang, Y., Sun, W., Dong, H., Li, Y., and Hu, J. (2020).
Dexmedetomidine Activation of Dopamine Neurons in the Ventral Tegmental Area Attenuates
the Depth of Sedation in Mice. Anesthesiology 133, 377-392.

Lefevre, E.M., Pisansky, M.T., Toddes, C., Baruffaldi, F., Pravetoni, M., Tian, L., Kono, T.J.Y.,
and Rothwell, P.E. (2020). Interruption of continuous opioid exposure exacerbates drug-evoked
adaptations in the mesolimbic dopamine system. Neuropsychopharmacology 45, 1781-1792.

Wang, F., Zhang, J., Yuan, Y., Chen, M., Gao, Z., Zhan, S., Fan, C., Sun, W., and Hu, J. (2020).
Salience processing by glutamatergic neurons in the ventral pallidum. Science Bulletin 65, 389-
401.

Tsuda, M., Ueno, S., and Inoue, K. (1999b). In vivo pathway of thermal hyperalgesia by
intrathecal administration of alpha,beta-methylene ATP in mouse spinal cord: involvement of
the glutamate-NMDA receptor system. Br J Pharmacol 127, 449-456.

Koshimizu, T.A., Honda, K., Nagaoka-Uozumi, S., Ichimura, A., Kimura, I., Nakaya, M., Sakai,
N., Shibata, K., Ushijima, K., Fujimura, A., et al. (2018). Complex formation between the
vasopressin 1b receptor, β-arrestin-2, and the μ-opioid receptor underlies morphine tolerance.
Nat Neurosci 21, 820-833.

Shu, H., Arita, H., Hayashida, M., Sekiyama, H., and Hanaoka, K. (2006). Effects of processed
Aconiti tuber and its ingredient alkaloids on the development of antinociceptive tolerance to
morphine. J Ethnopharmacol 103, 398-405.

Zhang, M., Dong, L., Zou, H., Li, J., Li, Q., Wang, G., and Li, H. (2018). Effects of Cannabinoid
Type 2 Receptor Agonist AM1241 on Morphine-Induced Antinociception, Acute and Chronic
Tolerance, and Dependence in Mice. J Pain 19, 1113-1129.

Chen, C., Zhang, J., Sun, L., Zhang, Y., Gan, W.B., Tang, P., and Yang, G. (2019). Long-term
imaging of dorsal root ganglia in awake behaving mice. Nat Commun 10, 3087.

Young, E.E., Bryant, C.D., Lee, S.E., Peng, X., Cook, B., Nair, H.K., Dreher, K.J., Zhang, X.,
Palmer, A.A., Chung, J.M., et al. (2016). Systems genetic and pharmacological analysis
identifies candidate genes underlying mechanosensation in the von Frey test. Genes Brain

Behav 15, 604-615.

Chaplan, S.R., Bach, F.W., Pogrel, J.W., Chung, J.M., and Yaksh, T.L. (1994). Quantitative assessment of tactile allodynia in the rat paw. J Neurosci Methods 53, 55-63.

McCoy, E.S., Taylor-Blake, B., Street, S.E., Pribisko, A.L., Zheng, J., and Zylka, M.J. (2013). Peptidergic CGRPα primary sensory neurons encode heat and itch and tonically suppress sensitivity to cold. Neuron 78, 138-151.

Yuan, Y., Wu, W., Chen, M., Cai, F., Fan, C., Shen, W., Sun, W., and Hu, J. (2019). Reward Inhibits Paraventricular CRH Neurons to Relieve Stress. Curr Biol 29, 1243-1251.e1244.